Spectrochimica Acta Part A: Molecular and Biomolecular Spectroscopy 269 (2022) 120759

Contents lists available at ScienceDirect

Spectrochimica Acta Part A: Molecular and Biomolecular Spectroscopy

journal homepage: www.elsevier.com/locate/saa

An amplified fluorescence polarization assay for sensitive sensing of organophosphorus pesticides via MnO_2 nanosheets

Yingfeng Qin [a,b,1], Gaojie Ye [b,1], Hao Liang [a], Ming Li [a], Jingjin Zhao [a]

[a] Key Laboratory of Ecology of Rare and Endangered Species and Environmental Protection (Guangxi Normal University), Ministry of Education, Guilin 541004, PR China
[b] Guangxi Key Laboratory of Bioactive Molecular Research and Evaluation, School of Basic Medical Sciences & Pharmaceutical College, Guangxi Medical University, Nanning 530021, PR China

HIGHLIGHTS

- A simple fluorescence polarization assay for sensitive and selective detection of organophosphorus pesticides was developed.
- This method showed good selectivity through the inhibition of AChE and reduction of MnO_2 nanosheets by TCh.
- Using MnO_2 nanosheets as mass amplifiers, there was a big difference in FP signal with a low LOD.
- This method displayed a good assay performance in real water samples.

GRAPHICAL ABSTRACT

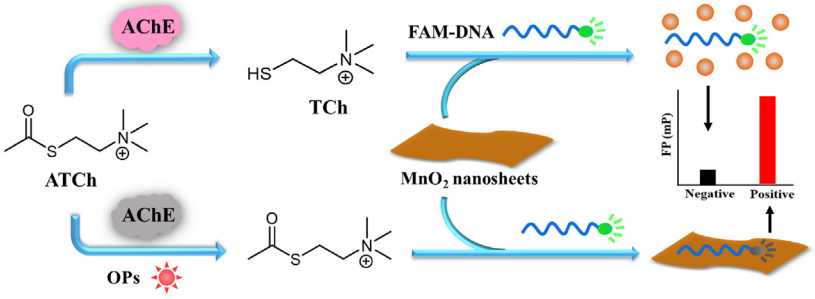

ARTICLE INFO

Article history:
Received 5 November 2021
Received in revised form 7 December 2021
Accepted 11 December 2021
Available online 22 December 2021

Keywords:
Fluorescence polarization
Organophosphorus pesticides
Acetylcholinesterase
MnO_2 nanosheets

ABSTRACT

It is highly desirable to develop a simple, efficient and sensitive strategy for organophosphorus pesticides (OPs) in both environment pollution and human health. Herein, a novel amplified fluorescence polarization (FP) biosensor was established for highly sensitive detection of OPs using MnO_2 nanosheets as the signal enhancer. In this system, OPs can suppress the activity of acetylcholinesterase (AChE) efficiently, blocking the hydrolysis reaction of acetylthiocholine (ATCh) to generate thiocholine (TCh) by AChE. TCh can lead the decomposition of MnO_2 nanosheets to manganese ions. So, without the influence of TCh, MnO_2 nanosheets can maintain its original shape and form a stable complex with FAM-DNA, which greatly enhanced the FP signal. This method can tremendously improve the sensitivity of FP with a detection limit of 0.01 ng/mL for diazinon. In addition, it was also applicable to determine other four OPs and investigate the level of diazinon in real water samples. Consequently, the proposed approach provides a new promising platform for detection of OPs and is expected to be used in application of environmental monitoring.

1. Introduction

As a typical pesticide, organophosphorus pesticides (OPs) have been widespread applied for agriculture industry to improve crop yields and products quality [1]. However, the abuse of OPs has caused serious food and environment pollution [2,3]. Most importantly, OPs have acute toxic which pose serious threats to human health due to its irreversible inhibition to acetylcholinesterase (AChE) [4,5]. Therefore, the accurate determination of OPs is of great significance for the management of pesticide contamination. Conventional chromatographic methods [6,7], which require expensive instruments and well trained operators, showing some

[1] These two authors contributed equally to this work.

https://doi.org/10.1016/j.saa.2021.120759
1386-1425/

limitations in OPs detection. The biosensors have greatly promoted the development of OPs accurate detection due to a number of key advantages, such as simple operation, low cost and in situ measurement [8]. Up to now, great efforts have been made to develop biosensors for the sensitive and selective determination of OPs [9–11]. However, developing a simple, sensitive method for quantification of OPs is still challenging but urgently needed.

Fluorescence polarization (FP) technique is a fascinating tool in a variety of fields, such as clinical diagnosis, biochemical, food safety, and environmental sensing [12–15]. Intriguingly, FP is insensitive to fluorophores concentration, but they are highly dependent on molecular volume or molecular weight of the fluorophores complex. Larger molecules with lower rates of rotation give higher FP values, while smaller molecules with higher rates of rotation usually weaker FP values [16]. Thus, to further improve the sensitivity of FP technique, mass-augmented amplification strategies can be used to increase the molecular size changes of fluorescent probes and to generate the amplify FP signal. These strategies have included macromolecules (proteins and oligonucleotides), and nanomaterials[17–19]. Our group has developed some nanomaterial-assisted FP methods in the detection of metal ion and nucleic acid [20,21].

MnO_2 nanosheets, one kind of 2D nanomaterials, are excellent nanoquenchers, catalysts, and adsorbents [22–24]. First, MnO_2 nanosheets can efficiently adsorb ssDNA by physisorption [25]. The adsorption properties allow MnO_2 nanosheets to acts as a FP enhancer. Zhang group explored a new fluorescence polarization method for sensitive detection of Ag^+ based on MnO_2 nanosheet-assisted ligand-DNA interaction [26]. In addition, compared with most of other 2D nanosheets, MnO_2 nanosheets have a strong oxidation ability and can be reduced to Mn^{2+} by some organic compounds. Such a property can also be used to constitute sensing strategies for practical applications [27,28]. However, despite a variety of MnO_2 nanosheets-based nanosensing platforms have been developed,[29] FP amplification technology based on MnO_2 nanosheets has seldom been studied.

Enlightened by the aforementioned works, a FP amplification method for OPs detection via AChE and MnO_2 nanosheets has been developed. Normally, AChE can catalyze the hydrolysis reaction of acetylthiocholine (ATCh) to generate thiocholine (TCh). And MnO_2 nanosheets can be decomposed to Mn^{2+} by TCh. OPs can suppress the activity of AChE which prevented the production of TCh, keeping MnO_2 nanosheets stay in its original shape. Then, the ssDNA modified with a fluorescent probe (F-DNA) can be effectively adsorbed by MnO_2 nanosheets aiming to a significant increase of FP value. Relying on AChE and MnO_2 nanosheets, the proposed FP amplification strategy provides good selectivity and high sensitivity for the detection of OPs.

2. Experimental

2.1. Chemicals and reagents

Organophosphorus pesticides (such as diazinon, paraoxon-methyl, omethoate, chlorpyrifos, and dichlorvos), other pesticide (such as acetamiprid, endosulfan, deltamethyrin, polyvinyl chloride), tetramethylammonium hydroxide (TMA.OH) and manganese chloride tetrahydrate ($MnCl_2{\cdot}4H_2O$) were purchased from Aladdin Industrial Corporation. Acetylcholinesterase (AChE) and acetylthiocholine (ATCh) were gained from Sigma-Aldrich. The oligonucleotides (F-DNA:5′-FAM-GCT AGG TTC AGGTCA C-3′) used in this work were synthesized by Shanghai Sangon Biotech Co. Ltd (Shanghai, China) and purified HPLC. All aqueous solutions were prepared with ultrapure water (18.2 MΩ·cm). The real river samples were obtained from Xiangsi river in Guilin City.

2.2. Instrumentation

FP measurements were performed by Cary Eclipse G9800A fluorimeter (Agilent Technologies, USA) with the excitation wavelength at 480 nm and the emission wavelength at 520 nm. The UV–vis spectra were collected by Cary 300 UV–vis spectrometer (Agilent Technologies, USA). Transmission electron microscopy (TEM) images were measured by a JEM-2100 HC transmission electron microscope (JEOL, Japan). Xray photoelectron spectroscopy (XPS) data were measured using an AXIS-ULTRA DLD electron spectrometer (Kratos, UK), High-performance liquid chromatography (HPLC) analyses were recorded on the Agilent 1260 LC system (Agilent Technologies, USA)

2.3. Preparation of MnO_2 nanosheets

The MnO_2 Nanosheets were synthesized according to the previous method with minor modifications [30]. In a typical synthesis process, 20 mL of a mixed aqueous solution of 600 mM TMA·OH and 3 wt% H_2O_2 was added to 10 mL of 300 mM $MnCl_2{\cdot}4H_2O$ aqueous solution within 15 s. The solution became dark brown immediately as the mixed aqueous solution added. Then, the mixed solution was vigorously stirred overnight in the ambient atmosphere at room temperature. After this mild oxidation process, the precipitate was washed with water and methanol and centrifuged (2000 rpm) for 20 mins, after which the precipitate was dried in a vacuum oven at 60 °C. 10 mg of bulk MnO_2 was added to 20 mL of water for ultrasonic treatment using ultrasonic cell disruption system. After ultrasonic treatment for 40 min, the dispersion was centrifuged at 1000 rpm to remove the un-exfoliated residues. Finally, the MnO_2 Nanosheets solution was stored at 4 °C for further research.

2.4. Detection procedure for OPs

First, 4 μL of 0.2 U/mL AChE, 2 μL of different concentrations of OPs, and 1 × Tris-HCl buffer (10 mM Tris-HCl (pH 7.9), 50 mM NaCl, 10 mM $MgCl_2$) incubated at 37 ℃ for 40 min with a total volume of 20 μL. Then 3 μL of 50 mM ATCh and 1 × Tris-HCl buffer were added and incubated for 30 min at 37 °C. Next, 12 μL of 30 μg/mL MnO_2 nanosheets was added for 20 min at room temperature. Finally, 3 μL FAM-DNA (0.5 μM) was added to the above mixture solution and incubated for 15 min at room temperature with a total volume of 150 μL. FP measurements were conducted at room temperature. All results of FP value measurements were represented in millipolarization (mP) units.

2.5. HPLC analysis

HPLC analyses were conducted on the Agilent 1260 LC system with autosampler. An Agilent TC-C18 4.6 × 250 mm column was used for separation. The column temperature was held constant at 30 °C. HPLC separation was achieved using isometric elution at a mobile phase (Methanol/H_2O, 75/25 v/v) flow rate of 1 mL/min for 15 min. The injection volume of samples was 20 μL. The chromatographic data of samples were recorded at 230 nm by using a diode array detector. The peaks of OPs in the real samples were identified by comparison with the retention time of standards. The samples were measured three times.

3. Results and discussion

3.1. Characterization of and MnO_2 nanosheets

The MnO_2 nanosheets synthesized were first characterized by TEM, UV–vis spectroscopy, and XPS. TEM pattern indicated that

the as-prepared MnO_2 nanosheets were two-dimensional thin-lamellar structure (Fig. 1A). The UV–vis spectra showed that the MnO_2 nanosheets had a broad band with a maximum absorption at 380 nm (Fig. 1B), which are consistent with the previous report. The aqueous solution of MnO_2 nanosheets showed stable dispersions, no precipitate appeared even after the dispersion was stored for more than two months (inset of Fig. 1B). According to the Mn 2p spectrum of XPS (Fig. 1C), two strong peaks were observed at 642.1 and 654.1 eV, which were attributed to Mn2p3/2 and Mn2p1/2 of MnO_2, respectively. Therefore, these characterization results showed that the MnO_2 nanosheets had been successfully prepared.

3.2. Principle of the sensing platform

The principle of the developed fluorescence polarization sensing platform for OPs quantification is described in Fig. 2. It has been reported that MnO_2 nanosheets can be used to enhance the fluorescence polarization signal [26]. In our previous work, [31] the change of FP value when labeled-ssDNA was adsorbed on nanosheets was demonstrated. Due to the formation a larger mass complex of ssDNA and nanosheets, such two-dimensional nanosheet can be used as an effective signal amplifier in FP detection methods. In this system, the MnO_2 nanosheets have dual functions, not only the FP enhancer, but also the recognizer of intermediate product TCh. Normally, AChE catalyzes the hydrolysis reaction of ATCh to generate TCh, which could be recognized by MnO_2 nanosheets and consume the nanosheets through sulfhydryl of TCh. And then, the MnO_2 nanosheets were reduced to Mn^{2+} which unable to adsorb FAM-DNA (employed as the fluorescence reporter, F-DNA), leading a low FP value without OPs in the system. However, upon the addition of OPs, the activity of AChE was inhibited efficiently. The hydrolysis of ATCh and the generation of TCh were impeded as well. Thus, F-DNA was adsorbed on the surface of MnO_2 nanosheets to form a F-DNA-MnO_2 nanosheets complex, resulting in a high FP signal due to the enlargement of the molecular volume with slow rotation. In light of the variation in FP values, quantitative analysis of organophosphorus pesticides can be performed.

3.3. Study of feasibility

The feasibility of the MnO_2 nanosheets-based fluorescence polarization strategy was evaluated by detecting diazinon, which is adopted as the OPs model analyte. As depicted in Fig. 3, the FP values of separate F-DNA (column A) or the mixture sample of ATCh, AChE and OPs (column B and C) were low and almost no obvious change. However, when MnO_2 nanosheets were introduced to the system, F-DNA was adsorbed on the surface of MnO_2 nanosheets, the FP value increased significantly due to the enlargement of the molecular volume (column D). The FP value drops rapidly after AChE and ATCh were added (column E), which was attributed to consumption of the large amounts of MnO_2 nanosheets by the products of AChE and ATCh reaction. After the introduction of OPs, the FP value was increased which meant that the OPs inhibited activity of AChE (column F). These abovementioned results clearly indicated the feasibility of the proposed assay.

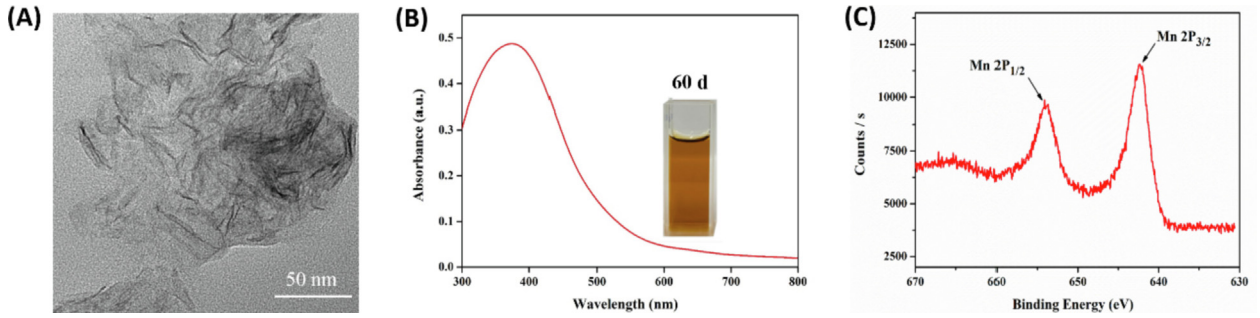

Fig. 1. The characterization of the MnO_2 nanosheets. (A) TEM image; (B) UV–vis absorption spectrum. Inset: the photos of the MnO_2 nanosheets dispersion in water; (C) XPS analysis.

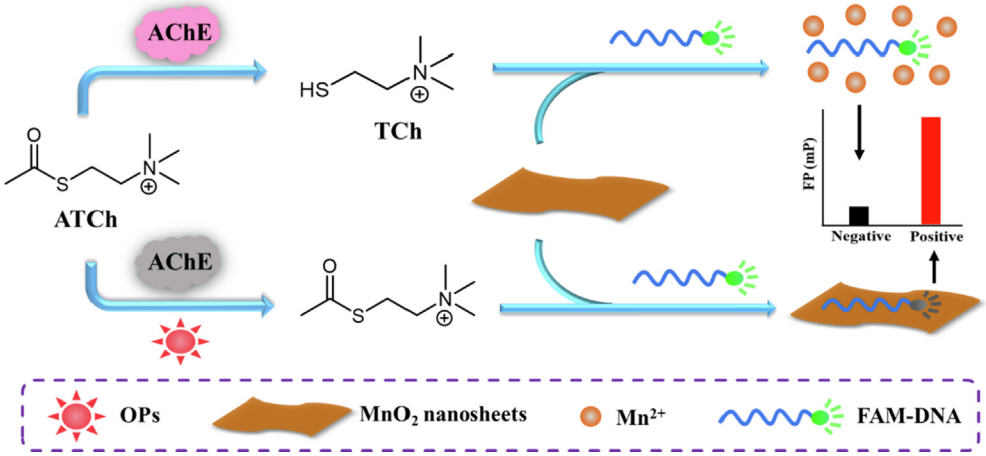

Fig. 2. Schematic illustration of the fluorescence polarization strategy based on the MnO_2 nanosheets and AChE for the detection of OPs.

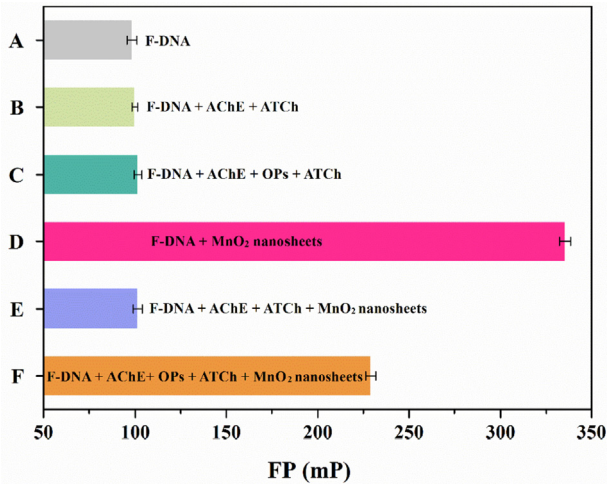

Fig. 3. The FP signal response obtained at different conditions.

3.4. Optimization of assay conditions

To obtain optimal performance of the proposed assay, some important experimental parameters were optimized. As dual functions of recognizer and FP enhancer, the concentration of MnO_2 nanosheets is a vital factor for assay performance and was first investigated. As shown in Fig. S1A, the FP value gradually increased and then reached saturation at 2.4 μg/mL as the MnO_2 nanosheets concentration increased. Thus, 2.4 μg/mL of MnO_2 nanosheets was chosen for further experiments. In addition, the MnO_2 nanosheets/F-DNA incubation time and the stability of MnO_2 nanosheets which enhance FP were also studied. As shown in Fig. S1B, the incubation time of MnO_2 nanosheets/F-DNA reaches equilibrium within 15 min. No remarkable changes of FP value were detected (Fig. S1C), indicating that the enhancement of FP by MnO_2 nanosheets can remain stable. The amount of AChE is another key factor for assay sensitivity. As shown in Fig. S1D, the FP value decreased when the concentration of AChE increased from 0 to 5.3 mU/mL and tends to level off at 5.3 mU/mL. This result indicated that the MnO_2 nanosheets were almost completely consumed by TCh which the product of AChE and ATCh reaction at 5.3 mU/mL of AChE. Thus, to obtain high sensitivity, the optimal AChE concentration was 5.3 mU/mL. In Fig. S1E, the FP value of the reaction time of AChE and ATCh obtained minimum at 30 min. Thus, 30 min was selected as the optimal reaction time of AChE and ATCh. Finally, in the presence of OPs, the incubation time of OPs and AChE was optimized. As shown in Fig. S1F, the FP signal increased with increasing incubation time and then reached a constant after 40 min. Thus, 40 min was chosen for the incubation time of OPs and AChE in this system.

3.5. Sensitive detection of diazinon

Diazinon is used as the OPs model analyte to study the analytical performance of the proposed FP sensor. Fig. 4 shows the FP signals of system to diazinon at different concentrations under optimal conditions. The FP signal strengthened gradually with diazinon concentration increasing (Fig. 4A), indicating that the FP sensor can be used for diazinon detection. A good linear relationship was obtained between △ FP and the logarithm of diazinon concentration in the range from 0.01 to 20 ng/mL (Fig. 4B). The detection limit was 0.01 ng/mL, which was lower than permissible concentrations in water and food samples. The detection limit and linear range of this FP assay is comparable or better than most of other existing methods, and a detailed comparison is shown in in Table 1 [32–38].

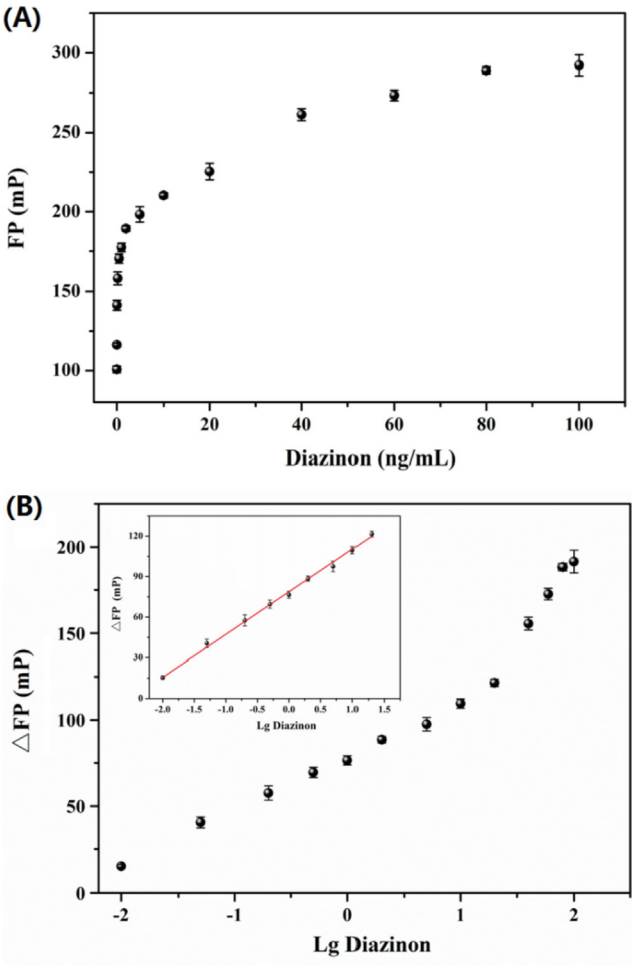

Fig. 4. (A) The FP signal response value with different concentrations of diazinon (0, 0.01, 0.05, 0.2, 0.5, 1, 2, 5, 10, 20, 40, 60, 80, 100 ng/mL). (B) The relationship between lg $C_{diazinon}$ and △FP. △FP = FP-FP_0, where FP and FP_0 represent the FP value with and without diazinon. Inset: linear curve for diazinon (0.01–20 ng/mL).

Table 1
Assay performance comparison between the proposed method and other methods for OPs detection.

Methods	Dynamic range (ng/mL)	Sensitivity (ng/mL)	Reference
Electrochemical aptasensor	0.0304–304	0.005	[32]
Chemiluminescence sensor	0.152–91.250	0.067	[33]
Fluorescence resonance energy transfer method	0.05–500	0.023	[34]
Corona discharge ion mobility spectrometry method	1.0–250	0.3	[35]
Fluorescence paper analytical device method	5.0–200	1.6	[36]
Fluorescence and colorimetric biosensor	0.75–1.0 × 10^5	0.4	[37]
Gas chromatography-flame ionization detector	2.0–1000	0.2	[38]
FP assay	0.01–20	0.01	This work

3.6. Responses of other OPs and pesticides

To verify that the proposed FP sensor could be used for detection of other OPs, the FP signal responses to other common OPs such as omethoate, paraoxon-methyl, chlorpyrifos and dichlorvos were studied. As seen in Fig. 5A, the remarkable increases in FP sig-

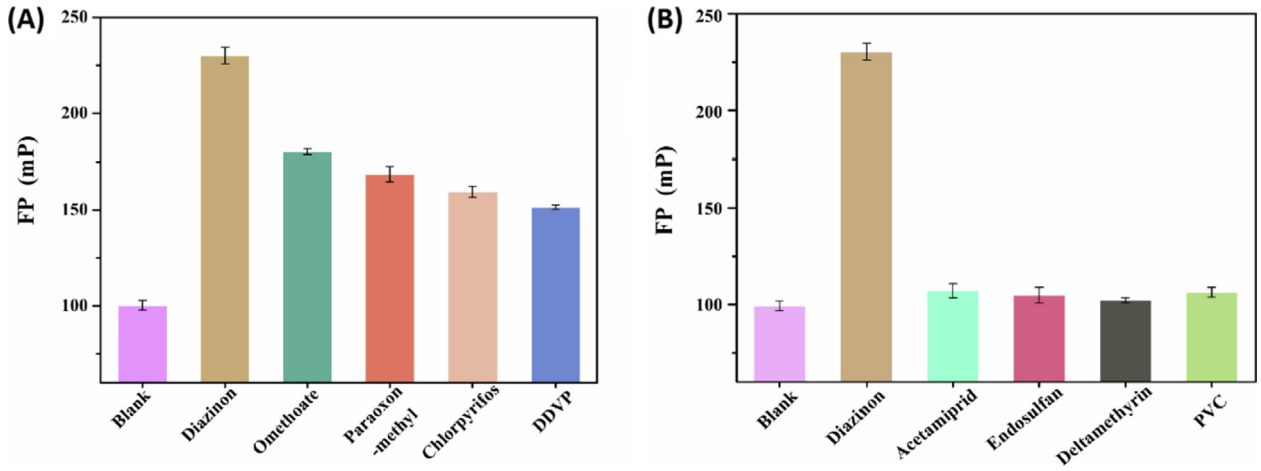

Fig. 5. (A) The FP signal response of different OPs. The concentrations of OPs were 20 ng/mL. (B) Selectivity of OPs detection. The concentration of diazinon was 20 ng/mL, the concentrations of other pesticides were 0.5 μg/mL.

Table 2
Detection diazinon in real water samples.

Samples	Added (ng/mL)	Found (ng/mL)	Recovery (%)	RSD (%, n = 3)	HPLC found (ng/mL)
1	0.200	0.207	103.5	3.8	–
2	1.000	0.984	98.4	2.7	1.023
3	5.000	5.014	100.3	3.4	4.976
4	15.000	14.427	96.2	2.3	14.733

nal of the system were also observed in the presence of other common OPs. These results demonstrated the proposed method could be generally applied for detection of OPs.

To evaluate the selectivity of the proposed FP strategy for OPs detection, the effects of four other pesticides (acetamiprid, endosulfan, deltamethyrin, polyvinyl chloride) were measured. The concentrations of other pesticides were 0.5 μg/mL, while the concentration of diazinon was 20 ng/mL. As Fig. 5B shown, a high FP signal was clearly observed in the presence of diazinon. However, there were negligible changes after the addition of other pesticides. Thus, the prepared FP sensor displayed high selectivity for OPs detection.

3.7. Detection of OPs in water samples

To demonstrate the practicability of the developed method, diazinon of various concentrations were added into river water samples to carry out the recovery experiment. Then, diazinon concentrations were detected by both the developed method and HPLC assay. As seen in Table 2, the results were similar to those of HPLC and the recoveries of diazinon in water samples were from 96.2% to 103.5%, demonstrating that the developed method possessed good performance for OPs in real samples.

4. Conclusions

In summary, a novel FP platform for the effective detection of OPs by using AChE inhibition and dual functional MnO_2 nanosheets was developed. As far as we know, it is the first time that MnO_2 nanosheets were used to construct a FP sensor for the detection of OPs. This method showed good selectivity through the inhibition of AChE and reduction of MnO_2 nanosheets by TCh. Moreover, with the MnO_2 nanosheets-assisted amplification, the sensitivity of the present method was substantially improved with a low detection limit of 0.01 ng/mL for diazinon, which was lower than most reported assays. In addition, this platform has advantages of good stability and low cost, providing a novel sensing pathway for OPs detection and shows great potential in practical applications.

CRediT authorship contribution statement

Yingfeng Qin: Methodology, Data curation, Writing – original draft. **Gaojie Ye:** Formal analysis, Writing – review & editing. **Hao Liang:** Formal analysis, Data curation, Investigation. **Ming Li:** Formal analysis, Validation. **Jingjin Zhao:** Conceptualization, Funding acquisition, Resources, Supervision, Writing – review & editing.

Declaration of Competing Interest

The authors declare that they have no known competing financial interests or personal relationships that could have appeared to influence the work reported in this paper.

Acknowledgement

This work was supported by y the National Natural Science Foundation of China (No. 21765003, 21966009) and Youth Science Foundation of Guangxi Medical University (GXMUYSF202104).

Appendix A. Supplementary material

Supplementary data to this article can be found online at https://doi.org/10.1016/j.saa.2021.120759.

References

[1] J. Kaushal, M. Khatri, S.K. Arya, A treatise on organophosphate pesticide pollution: current strategies and advancements in their environmental degradation and elimination, Ecotox. Environ. Safe. 207 (2021) 111483.
[2] P. Kumar, K.-H. Kim, A. Deep, Recent advancements in sensing techniques based onfunctional materials for organophosphate pesticides, Biosens. Bioelectron. 70 (2015) 469–481.

[3] R. Jayaraj, P. Megha, P. Sreedev, Organochlorine pesticides, their toxic effects on living organisms and their fate in the environment, Interdiscip. Toxicol. 9 (3–4) (2016) 90–100.
[4] A. Chanda, S.K. Khetan, D. Banerjee, A. Ghosh, T.J. Collins, Total degradation of fenitrothion and other organophosphorus pesticides by catalytic oxidation employing Fe-TAML peroxide activators, J. Am. Chem. Soc. 128 (37) (2006) 12058–12059.
[5] D.M. Quinn, Acetylcholinesterase: enzyme structure, reaction dynamics, and virtual transition states, Chem. Rev. 87 (1987) 955–979.
[6] C. Hu, M. He, B. Chen, B. Hu, A sol-gel polydimethylsiloxane/ polythiophene coated stir bar sorptive extraction combined with gas chromatography-flame phcrtometric detection for the determination of organophosphoms pesticides in environmental water samples, J. Chromatogr. A. 1275 (2013) 25–31.
[7] J. Lee, H.K. Lee, Fully automated dynamic in-syringe liquid-phase microextraction and on-column derivatization of carbamate pesticides with gas chromatography/mass spectrometric analysis, Anal. Chem. 83 (17) (2011) 6856–6861.
[8] A.K. Wanekaya, W. Chen, A. Mulchandani, Recent biosensing developments in environmental security, J. Environ. Monitor. 10 (6) (2008) 703–712.
[9] B. Wang, H. Wang, X. Zhong, Y. Chai, S. Chen, R. Yuan, A highly sensitive electrochemiluminescence biosensor for the detection of organophosphate pesticides based on cyclodextrin functionalized graphitic carbon nitride and enzyme inhibition, Chem. Commun. 52 (28) (2016) 5049–5052.
[10] J. Perumal, Y. Wang, A.B.E. Attia, U.S. Dinish, M. Olivo, Towards a point-of-care SERS sensor for biomedical and agri-food analysis applications: a review of recent advancements, Nanoscale 13 (2021) 553–580.
[11] B. Liang, L. Han, Displaying of acetylcholinesterase mutants on surface of yeast for ultra-trace fluorescence detection of organophosphate pesticides with gold nanoclusters, Biosens. Bioelectron. 148 (2019) 111825.
[12] Z. Zhang, C. Tang, L. Zhao, L.i. Xu, W. Zhou, Z. Dong, Y. Yang, Q. Xie, X. Fang, Aptamer-based fluorescence polarization assay for separation-free exosome quantification, Nanoscale 11 (20) (2019) 10106–10113.
[13] H. Zhang, S. Yang, K. De Ruyck, N.V. Beloglazova, S.A. Eremin, S. De Saeger, S. Zhang, J. Shen, Z. Wang, Fluorescence polarization assays for chemical contaminants in food and environmental analyses, TrAC-Trend Anal. Chem. 114 (2019) 293–313.
[14] J.W. Choi, G.J. Kim, S. Lee, J. Kim, A.J. deMello, S. Chang, A droplet-based fluorescence polarization immunoassay (dFPIA) platform for quantitative analysis of protein biomarker, Biosens. Bioelectron. 67 (2015) 497–502.
[15] D.M. Jameson, J.A. Ross, Fluorescence polarization/anisotropy in diagnostics and imaging, Chem. Rev. 110 (5) (2010) 2685–2708.
[16] Q. Zhao, J. Tao, J.S. Uppal, H. Peng, H. Wang, X.C. Le, Nucleic acid aptamers improving fluorescence anisotropy and fluorescence polarization assays for small molecules, TrAC-Trend Anal. Chem. 110 (2019) 401–409.
[17] Y. Gao, J. Xu, B. Li, Y. Jin, Nanoparticles-aided amplification of fluorescence polarization for ultra-sensitively monitoring activity of telomerase, ACS Appl. Mater. Inter. 8 (2016) 13707–13713.
[18] L. Qi, Y.-Y. Fan, H.e. Wei, D. Zhang, Z.-Q. Zhang, Graphene oxide-enhanced and proflavine-probed fluorescence polarization biosensor for ligand-RNA interaction assay, Sensor Actuat. B-Chem. 257 (2018) 666–671.
[19] Y.-C. He, B.-C. Yin, L. Jiang, B.-C. Ye, The rapid detection of microrna based on p19-enhanced fluorescence polarization, Chem. Commun. 50 (47) (2014) 6236–6239.
[20] S. Liao, J. Zhao, Y. Qin, S. Zhao, A novel fluorescence polarization assay for copper ions based on DNA-templated click chemistry and amplification of nanoparticles, RSC Adv. 7 (88) (2017) 55668–55672.
[21] J. Zhao, Z. Chu, X. Jin, S. Zhao, A fluorescence polarization assay for nucleic acid based on the amplification of hybridization chain reaction and nanoparticles, Sensor Actuat. B-Chem. 209 (2015) 116–121.
[22] W. Zhai, C. Wang, P. Yu, Y. Wang, L. Mao, Single-layer MnO_2 nanosheets suppressed fluorescence of 7-hydroxycoumarin: mechanistic study and application for sensitive sensing of ascorbic acid in vivo, Anal. Chem. 86 (2014) 12206–12213.
[23] J. Liu, L. Meng, Z. Fei, P.J. Dyson, X. Jing, X. Liu, MnO_2 nanosheets as an artificial enzyme to mimic oxidase for rapid and sensitive detection of glutathione, Biosens. Bioelectron. 90 (2017) 69–74.
[24] Y. Yao, N. Li, X. Zhang, J.O. Machuki, D. Yang, Y. Yu, J. Li, D. Tang, J. Tian, F. Gao, DNA-templated silver nanocluster/porphyrin/MnO_2 platform for label-free intracellular Zn^{2+} imaging and fluorescence-/magnetic resonance imaging-guided photodynamic therapy, ACS Appl. Mater. Inter. 11 (2019) 13991–14003.
[25] Z. Zhao, H. Fan, G. Zhou, H. Bai, H. Liang, R. Wang, X. Zhang, W. Tan, Activatable fluorescence/MRI bimodal platform for tumor cell imaging via MnO_2 nanosheet-aptamer nanoprobe, J. Am. Chem. Soc. 136 (32) (2014) 11220–11223.
[26] L. Qi, Z. Yan, Y. Huo, X.-M. Hai, Z.-Q. Zhang, MnO_2 nanosheet-assisted ligand-DNA interaction-based fluorescence polarization biosensor for the detection of Ag^+ ions, Biosens. Bioelectron. 87 (2017) 566–571.
[27] H. Fan, Z. Zhao, G. Yan, X. Zhang, C. Yang, H. Meng, Z. Chen, H. Liu, W. Tan, A smart DNAzyme-MnO_2 nanosystem for efficient gene silencing, Angew. Chem. Int. Ed. 54 (16) (2015) 4801–4805.
[28] T. Xiao, J. Sun, J. Zhao, S. Wang, G. Liu, X. Yang, FRET effect between fluorescent polydopamine nanoparticles and MnO_2 nanosheets and its application for sensitive sensing of alkaline phosphatase, ACS Appl. Mater. Inter. 10 (7) (2018) 6560–6569.
[29] J. Chen, H. Meng, Y. Tian, R. Yang, D. Du, Z. Li, L. Qu, Y. Lin, Recent advances in functionalized MnO_2 nanosheets for biosensing and biomedicine applications, Nanoscale Horiz. 4 (2) (2019) 321–338.
[30] L. Peng, X. Peng, B. Liu, C. Wu, Y. Xie, G. Yu, Ultrathin two-dimensional MnO_2/graphene hybrid nanostructures for high-performance, flexible planar supercapacitors, Nano Lett. 13 (2013) 2151.
[31] J. Zhao, Y. Ma, R. Kong, L. Zhang, W. Yang, S. Zhao, Tungsten disulfide nanosheet and exonuclease III co-assisted amplification strategy for highly sensitive fluorescence polarization detection of DNA glycosylase activity, Anal. Chim. Acta 887 (2015) 216–223.
[32] S. Hassani, M.R. Akmal, A. Salek-Maghsoudi, S. Rahmani, M.R. Ganjali, P. Norouzi, M. Abdollahi, Novel label-free electrochemical aptasensor for determination of Diazinon using gold nanoparticles-modified screen-printed gold electrode, Biosens. Bioelectron. 120 (2018) 122–128.
[33] N. Bagheri, A. Khataee, J. Hassanzadeh, L. Samaei, Highly sensitive chemiluminescence sensing system for organophosphates using mimic LDH supported ZIF-8 nanocomposite, Sensor Actuat. B-Chem. 284 (2019) 220–227.
[34] Y. Rong, H. Li, Q. Ouyang, S. Ali, Q. Chen, Rapid and sensitive detection of diazinon in food based on the FRET between rare-earth doped upconversion nanoparticles and graphene oxide, Spectrochim. Acta A 239 (2020) 118500.
[35] S. Amini, H. Ebrahimzadeh, S. Seidi, N. Jalilian, Preparation of Polyacrylonitrile/Ni-MOF electrospun nanofiber as an efficient fiber coating material for headspace solid-phase microextraction of diazinon and chlorpyrifos followed by CD-IMS analysis, Food Chem. 350 (2021) 129242.
[36] J. Chen, X. Chen, P.o. Wang, S. Liu, Z. Chi, Aggregation-induced emission luminogen@manganese dioxide core-shell nanomaterial-based paper analytical device for equipment-free and visual detection of organophosphorus pesticide, J. Hazard. Mater. 413 (2021) 125306, https://doi.org/10.1016/j.jhazmat.2021.125306.
[37] Y. Cai, H. Zhu, W. Zhou, Z. Qiu, C. Chen, A. Qileng, K. Li, Y. Liu, Capsulation of AuNCs with AIE effect into metal-organic framework for the marriage of a fluorescence and colorimetric biosensor to detect organophosphorus pesticides, Anal. Chem. 93 (19) (2021) 7275–7282.
[38] Z. Aladaghlo, A. Fakhari, M. Behbahani, Solvent-assisted dispersive solid-phase extraction: a sample preparation method for trace detection of diazinon in urine and environmental water samples, J. Chromatogr. A. 1462 (2016) 27–34.